Draft version September 7, 2016
Preprint typeset using LaTeX style emulateapj v. 12/16/11

arXiv:1609.00679v2 [astro-ph.SR] 6 Sep 2016

G64−12 AND G64−37 ARE CARBON-ENHANCED METAL-POOR STARS

Vinicius M. Placco[1,2], Timothy C. Beers[1,2],
Henrique Reggiani[3], Jorge Meléndez[3]

Draft version September 7, 2016

ABSTRACT

We present new high-resolution chemical-abundance analyses for the well-known high proper-motion subdwarfs G64−12 and G64−37, based on very high signal-to-noise spectra ($S/N \sim 700/1$) with resolving power $R \sim 95,000$. These high-quality data enable the first *reliable* determination of the carbon abundances for these two stars; we classify them as carbon-enhanced metal-poor (CEMP) stars based on their carbonicities, which both exceed [C/Fe] = +1.0. They are sub-classified as CEMP-no Group-II stars, based on their location in the Yoon-Beers diagram of absolute carbon abundance, A(C) vs. [Fe/H], as well as on the conventional diagnostic [Ba/Fe]. The relatively low absolute carbon abundances of CEMP-no stars, in combination with the high effective temperatures of these two stars ($T_{\rm eff} \sim 6500$ K) weakens their CH molecular features to the point that accurate carbon abundances can only be estimated from spectra with very high S/N. A comparison of the observed abundance patterns with the predicted yields from massive, metal-free supernova models reduces the inferred progenitor masses by factors of $\sim$ 2-3, and explosion energies by factors of $\sim$ 10-15, compared to those derived using previously claimed carbon abundance estimates. There are certainly many more warm CEMP-no stars near the halo main-sequence turnoff that have been overlooked in past studies, directly impacting the derived frequencies of CEMP-no stars as a function of metallicity, a probe that provides important constraints on Galactic chemical evolution models, the initial mass function in the early Universe, and first-star nucleosynthesis.

Keywords: Galaxy: halo—stars: abundances—stars: Population II—stars: individual (G64−12)—stars: individual (G64−37)

1. INTRODUCTION

The basic cosmological framework suggesting that the chemical evolution of the Universe is a continuous process of nucleosynthesis and mixing of subsequent stellar generations has been in place since the work of Hoyle (1954). In this scenario, the long-lived, low-mass extremely metal-poor (EMP; [Fe/H][4] < -3.0, e.g., Beers & Christlieb 2005; Frebel & Norris 2015) stars observed today were formed from gas that was polluted by the nucleosynthesis products of previous generations of (likely massive) stars, also known as Population III (Pop III). The proposed existence of massive Pop III stars is not new (e.g., Puget & Heyvaerts 1980); the first comparison between the theoretical yields of Pop III stars and observed elemental abundances of very metal-poor stars was made by Nomoto et al. (1999). Since then, there has been significant advances in our understanding of the underlying physics of first-generation stars, and different classes of models are able to well-reproduce observations of EMP stars in the Galaxy (see Placco et al. 2016, for a brief summary).

Despite the fact that the elemental-yield predictions of first-star nucleosynthesis differ somewhat between various authors, they all agree that the light element carbon plays a central role at early times. Indeed, the majority of the long-lived relics of the chemical evolution in the early Universe are expected to be heavy-metal deficient, but carbon enhanced (Frebel et al. 2007). Such stars, which once were considered an *Astrophysical Enigma* by Bidelman (1956)[5], today are known as carbon-enhanced metal-poor (CEMP) stars, following recognition of their existence at the lowest metallicities by Beers et al. (1992).

Although carbon-enhanced Solar-metallicity stars were first identified almost 75 years ago (Keenan 1942), the majority of early spectral catalogs contained only cooler ($T_{\rm eff} < 4500$ K) carbon stars with strong molecular features (Kamijo 1959). One of the first attempts to determine carbon abundances for warmer ($T_{\rm eff} > 5500$ K), low-metallicity stars came some twenty years later (Peterson & Sneden 1978). This study only considered stars of relatively higher metallicity ([Fe/H] > -2.3), since few stars were known below this abundance at the time. Nevertheless, it showed that, even when the carbon abundance ratio relative to iron (carbonicity; Placco et al. 2011) of a given star is high ([C/Fe] $> +1.0$), the CH molecular features around 4300 Å can be quite weak at these temperatures, present at less than 2% of the continuum level for $T_{\rm eff} = 6500$ K. As a result, reliable carbonicity determinations for warm stars are biased towards relatively bright stars, where the S/N required to detect such small deviations from the continuum can be obtained with reasonable integration times.

The recognition that carbon-enhanced stars occur with

[1] Department of Physics, University of Notre Dame, Notre Dame, IN 46556, USA
[2] JINA Center for the Evolution of the Elements, USA
[3] Departamento de Astronomia - Instituto de Astronomia, Geofísica e Ciências Atmosféricas, Universidade de São Paulo, São Paulo, SP 05508-900, Brazil

[4] [A/B] = $log(N_X/N_Y)_\star - \log(N_X/N_Y)_\odot$, where N is the number density of atoms of elements X and Y in the star ($\star$) and the Sun ($\odot$), respectively.

[5] The author states "*The spectra of these objects show extremely strong absorption features due to CH, and considerably weaker lines of neutral metals than do the typical carbon stars.*"

Table 1
Final Abundance Estimates for G64−12 and G64−37.

		G64−12				G64−37			
Ion	$\log \epsilon_\odot$ (X)	$\log \epsilon$ (X)	[X/H]	[X/Fe]	σ	$\log \epsilon$ (X)	[X/H]	[X/Fe]	σ
Li I	1.05	2.36	+1.31	+4.59	0.04	2.25	+1.20	+4.31	0.03
C (CH)	8.43	6.21	−2.22	+1.07	0.05	6.44	−1.99	+1.12	0.05
O I	8.69	6.58	−2.11	+1.17	0.07	6.59	−2.10	+1.00	0.03
Na I	6.24	2.87	−3.37	−0.09	0.03	2.92	−3.32	−0.21	0.03
Mg I	7.60	4.79	−2.80	+0.48	0.07	4.87	−2.73	+0.38	0.07
Al I	6.45	2.56	−3.90	−0.61	0.05	2.63	−3.82	−0.71	0.05
Si I	7.51	4.06	−3.45	−0.16	0.04	4.11	−3.40	−0.29	0.03
Ca I	6.34	3.56	−2.78	+0.50	0.03	3.64	−2.70	+0.41	0.03
Sc II	3.15	0.03	−3.12	+0.17	0.06	0.20	−2.95	+0.15	0.05
Ti I	4.95	2.40	−2.55	+0.74	0.05	2.53	−2.42	+0.69	0.04
Ti II	4.95	2.19	−2.76	+0.52	0.09	2.34	−2.61	+0.50	0.07
Cr I	5.64	2.27	−3.37	−0.09	0.05	2.50	−3.14	−0.03	0.04
Mn I	5.43	1.50	−3.93	−0.65	0.05	1.77	−3.66	−0.55	0.04
Fe I	7.50	4.21	−3.29	0.00	0.04	4.39	−3.11	0.00	0.03
Fe II	7.50	4.26	−3.24	+0.05	0.06	4.45	−3.05	+0.05	0.04
Co I	4.99	2.10	−2.89	+0.40	0.05	2.23	−2.76	+0.35	0.05
Ni I	6.22	2.95	−3.27	+0.02	0.03	3.17	−3.05	+0.06	0.02
Zn I	4.56	1.80	−2.76	+0.52	0.03	1.92	−2.64	+0.47	0.02
Sr II	2.87	−0.34	−3.21	+0.07	0.06	−0.19	−3.06	+0.05	0.04
Ba II	2.18	−1.17	−3.35	−0.07	0.06	−1.28	−3.46	−0.36	0.04

higher frequency at lower metallicities extends back over two decades (e.g., Beers et al. 1992, and references therein). Subsequent observations of metal-poor stars using medium- and high-resolution spectroscopy has confirmed that the fractions of CEMP stars increases from $\sim 15-20\%$ for [Fe/H] < -2.0 to more than 80% for [Fe/H] < -4.0 (Lee et al. 2013; Placco et al. 2014a), prima facia observational evidence that carbon is an important contributor to the chemical evolution of the early Universe.

Among the various sub-classes of CEMP stars (Beers & Christlieb 2005), the CEMP-no stars (which exhibit no enhancements in their neutron-capture elements, e.g., [Ba/Fe] < 0.0) are believed to have formed from gas polluted by the nucleosynthesis products of massive stars, perhaps including Pop III progenitors. Even though the low abundances of neutron-capture elements (such as Ba) is a feature of such stars, it has been recently suggested by Yoon et al. (2016), building on the work of Spite et al. (2013) and Bonifacio et al. (2015), that the absolute carbon abundance (A(C) = log ϵ(C)) is a sufficient (and likely more fundamental) criterion to distinguish CEMP-no stars from the far more populous sub-class of CEMP-s stars (where the carbon enhancement arises due to mass transfer from a binary asymptotic giant-branch stellar companion). This new criterion is particularly useful for warmer CEMP stars, where measurement of [Ba/Fe] can prove challenging.

In this paper, we present the first confirmation that the well-studied subdwarfs G64−12 and G64−37 are in fact CEMP-no stars. Even though these stars have been considered by numerous previous authors, accurate determinations of their carbon abundances was limited by the quality of the available spectra. It is highly likely that other warm low-metallicity stars have been incorrectly classified as "carbon-normal," a deficiency that must be addressed in the future. This paper is outlined as follows: Section 2 describes the spectroscopic data used in this work, and presents the elemental-abundance estimates obtained for G64−12 and G64−37 from our very high-quality data. Section 3 considers the consequences of properly classifying warm CEMP-no stars on our understanding the nature of their progenitors, and on the derived CEMP fractions as a function of metallicity. Our conclusions are provided in Section 4.

2. G64−12 AND G64−37: CEMP-NO STARS

G64−12 (Wolf 1492; $\alpha = 13^h40^m02^s.498$, $\delta = -00°02'18.80''$, $V = 11.45$) is a well-known, high proper-motion EMP subdwarf. It was first identified as such by Sandage (1969) and, since then, has been the target of 225 studies in the literature, according to the SIMBAD database. It also possesses an extremely high radial velocity ($V_r = 442.51 \pm 0.18$ km/s; Latham et al. 2002), and indeed has been used to obtain early estimates of the mass of the Galaxy from its derived rest-frame space velocity (Carney et al. 1988). Based on 33 radial-velocity measurements spanning 4818 days, Latham et al. (2002) concluded that G64−12 is not in a binary system. The full space motion of G64−12 estimated by Allen et al. (1991) clearly indicates that it is a member of the outer-halo population (Carollo et al. 2007; Beers et al. 2012); a high-energy retrograde orbit ($\Theta \sim -138$ km/s) with a maximum distance from the Galactic plane $Z_{\rm max} \sim 40$ kpc.

According to the SAGA database (Suda et al. 2008), there are 26 papers with estimated chemical abundances for G64−12. However, the carbonicity for this star is estimated by only four studies (Akerman et al. 2004; Barklem et al. 2005; Aoki et al. 2006; Zhang et al. 2011), with values ranging from [C/Fe] = +0.30 to [C/Fe] = +0.88. Most other studies either do not report an estimate of [C/Fe], or only obtain weak upper limits. In addition, Fabbian et al. (2009) derived the carbon abundance for G64−12 using C I features in the near-infrared, with a value of [C/Fe] = +0.53.

G64−37 (Ross 841; $\alpha = 14^h02^m30^s.091$, $\delta = -05°39'05.20''$, $V = 11.15$) is also an EMP subdwarf, recognized as a high proper-motion star decades before G64−12 (Ross 1930). Although it is well-studied, this star has fewer references in the literature than G64−12, 115 according to the SIMBAD database. Even though its

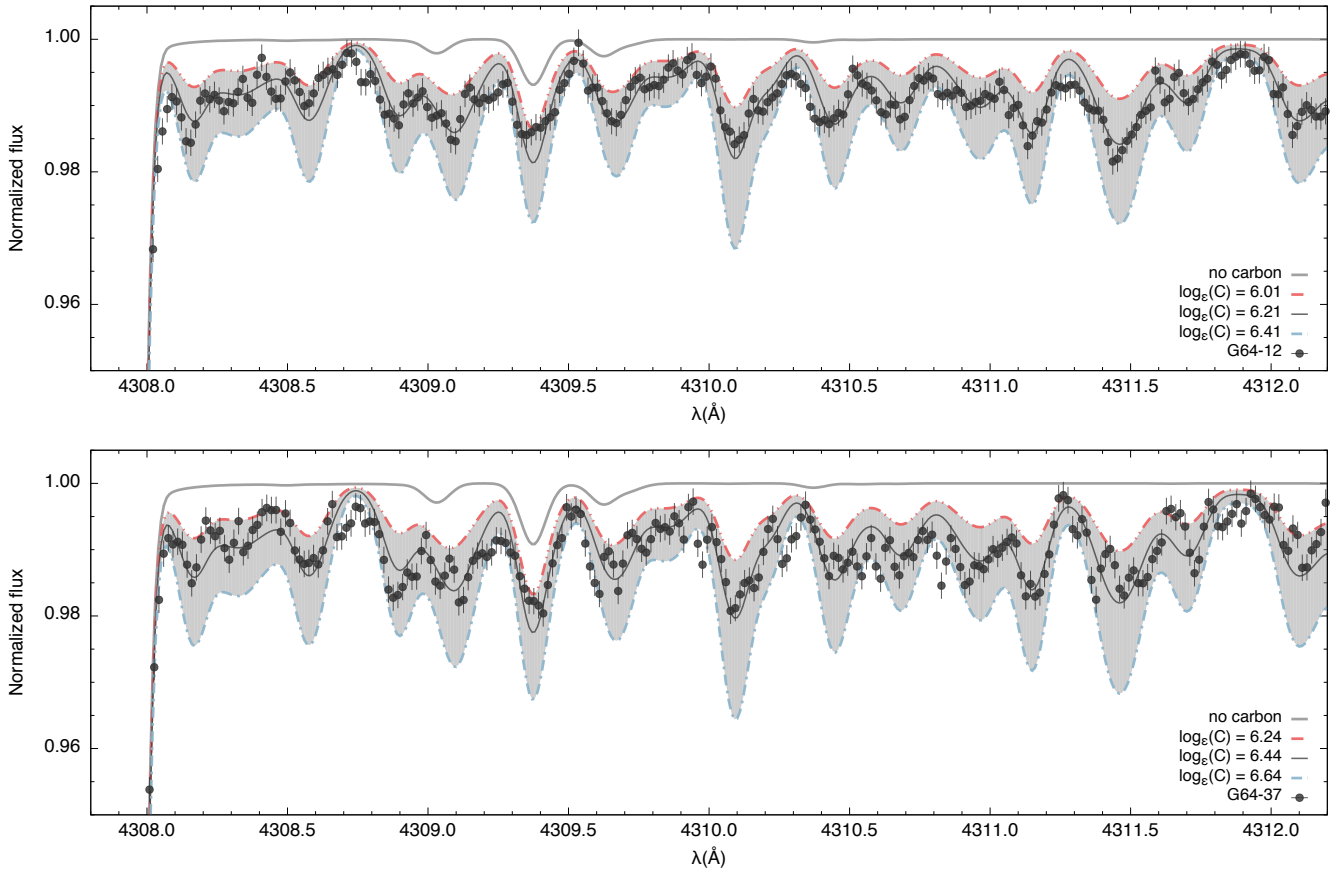

Figure 1. Spectral synthesis of the CH G-band for G64−12 (upper panel) and G64−37 (lower panel). The dots represent the observed spectra, the solid black lines are the best abundance fits, and the dotted and dashed lines are the lower and upper abundances, used to estimate the uncertainty. The shaded area encompasses a 0.4 dex difference in $\log\epsilon$(C). The light gray lines show the synthesized spectrum in the absence of carbon. Note the extremely small maximum deviation of the carbon features for both stars below the continuum, $\sim 1-2\%$.

radial velocity is lower ($V_r = 81.52 \pm 0.20$ km/s; Latham et al. 2002), its derived space motion also indicates clear membership in the outer-halo population. G64−37 is also considered a single star by Latham et al. (2002), based on 22 radial velocity measurements spanning 1938 days. Allen et al. (1991) obtain a high-energy retrograde orbit ($\Theta \sim -209$ km/s) with a maximum distance from the plane $Z_{\rm max} \sim 10-35$ kpc (according to these authors, the large errors in this estimate arise primarily from the sensitivity of its derived orbit to distance errors).

Elemental abundances for G64−37 are reported by 20 different studies, according to the SAGA database, but measurements of carbonicity are reported only by Akerman et al. (2004), [C/Fe] = +0.29, and Fabbian et al. (2009), [C/Fe] = +0.41.

The high-resolution spectra for G64−12 and G64−37 used in this work were obtained with the HIRES instrument on the Keck 10-m telescope at Mauna Kea. The resolving power of $R \sim 95,000$ and signal-to-noise ratio $S/N = 700/1$ at 5000 Å allowed for an elemental-abundance analysis of unprecedented precision for these two stars. The first high-quality differential abundance analysis of EMP stars, based on G64−12 and G64−37, was reported by Reggiani et al. (2016); their derived 1D, LTE abundances (which did not appear in the published work) are shown here for the first time. The abundances were measured using the semi-automated code q^2 (Ramírez et al. 2014), which communicates with the radiative transfer code MOOG (Sneden 1973).

The atmospheric parameters adopted for these stars are: G64−12 [$T_{\rm eff}$= 6463(50) K, log g= 4.26(0.15), [Fe/H]= −3.29(0.02), and ξ = 1.65(0.06) km/s]; G64−37 [$T_{\rm eff}$= 6570(27) K, log g= 4.40(0.06), [Fe/H]= −3.11(0.02), and ξ = 1.74(0.06) km/s]. The atmospheric parameters of G64−37 were calculated differentially, using the Fe lines from G64−12 as a reference. The errors for G64−12 come from the original sources of the atmospheric parameters (IRFM $T_{\rm eff}$ from Meléndez et al. 2010 and log g from Nissen et al. 2007, and the differential calculations for [Fe/H] and ξ from Reggiani et al. 2016). The errors for G64−37 were calculated differentially by varying the atmospheric parameters of G64−12. Table 1 lists the $\log\epsilon$ (X), [X/H], [X/Fe] abundances and uncertainties for 17 elements. The Solar elemental abundances of Asplund et al. (2009) were used.

In order to confirm the CEMP sub-classes of G64−12 and G64−37, the carbon and barium abundance ratios must be calculated via spectral synthesis. The linelist used for the carbon abundance determinations has CH data from Masseron et al. (2014), with a ^{12}C/^{13}C isotopic ratio of 4 to 5 indicated therein, and atomic data from the Kurucz linelists[6]. The final values are [C/Fe] = +1.07 and [Ba/Fe] = −0.07 for G64−12 and [C/Fe] = +1.12 and [Ba/Fe] = −0.36 for G64−37, satisfying the

[6] http://kurucz.harvard.edu/linelists.html

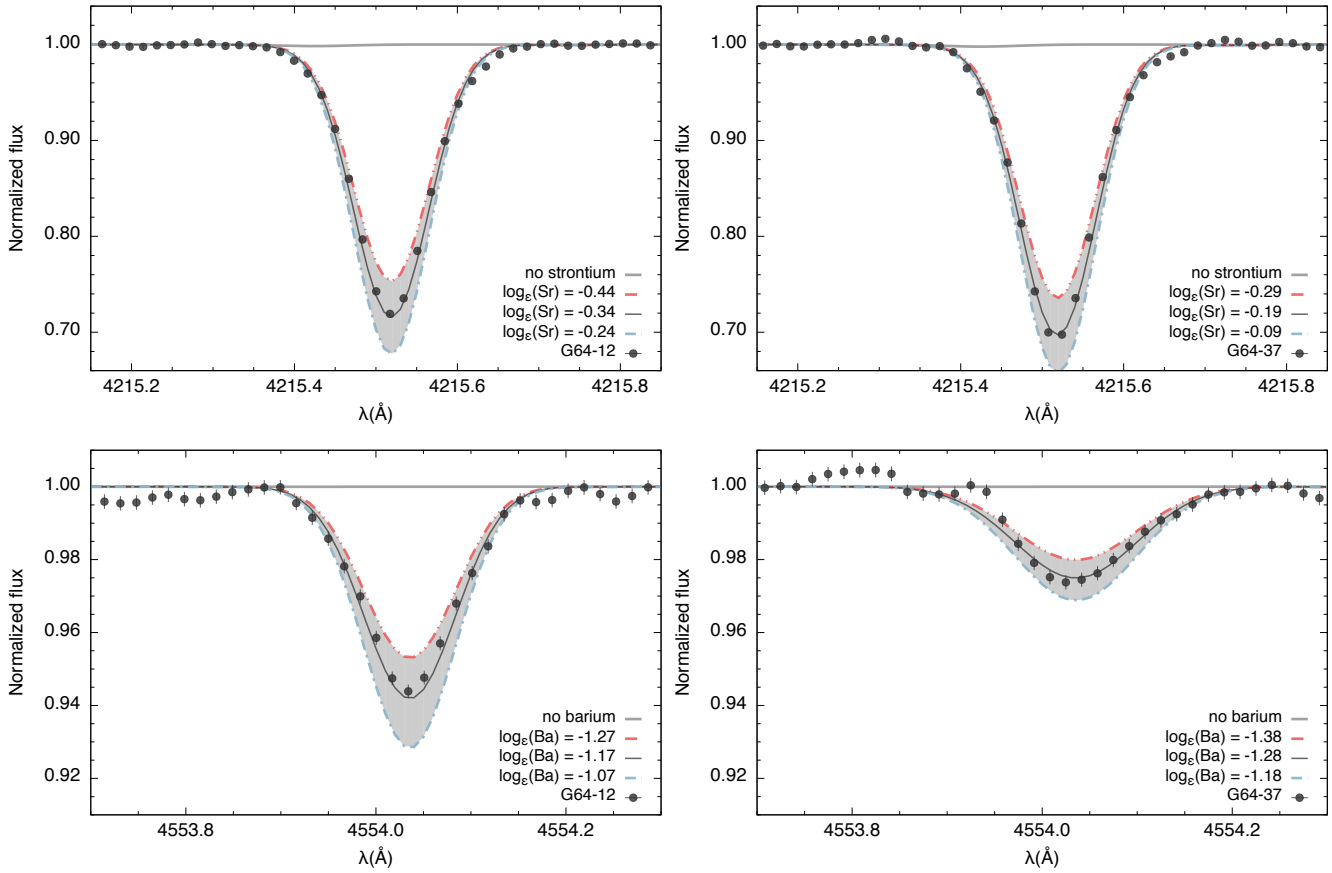

Figure 2. Spectral synthesis of the Sr II (upper panels) and Ba II (lower panels) features for G64−12 and G64−37. The dots represent the observed spectra, the solid black lines are the best abundance fits, and the dotted and dashed line are the lower and upper abundances, used to estimate the uncertainty. The shaded area encompasses a 0.2 dex difference in the abundances. The light gray line shows the synthesized spectrum in the absence of strontium and barium.

original definition for CEMP-no stars ([C/Fe] $>$ +1.0, [Ba/Fe] $<$ 0.0; Beers & Christlieb 2005). The atmospheric parameters errors have an effect of $\sim$ 0.02 dex on A(C), which does not affect the conclusions regarding the classification of these stars.

Figures 1 and 2 show, respectively, the spectral synthesis of the CH G-band molecular features and the Sr II (λ4215) and Ba II (λ4554) atomic features, for G64−12 and G64−37. The dots represent the observed spectra, the solid black lines are the best abundance fits, and the dotted and dashed lines are the lower and upper abundance limits, used to estimate the uncertainties in these determinations. The shaded area encompasses a 0.2-0.4 dex difference in the abundances. The light gray lines show the synthesized spectra in the absence of C, Sr, and Ba.

Both stars are also classified as CEMP-no stars by the A(C) criterion described in Yoon et al. (2016). Their values of A(C) = 6.21 (G64−12) and A(C) = 6.44 (G64−37), with metallicities of [Fe/H] = −3.29 and −3.11, respectively, place them among the CEMP-no Group-II stars in Figure 1 of Yoon et al. (the Yoon-Beers diagram), although G64−37 lies close to the CEMP-no Group-III region. However, based on their Na and Mg abundances, both these objects are clearly Group-II stars (see Figure 4 of Yoon et al.).

We note that the carbon abudances were determined from a 1D LTE analysis, and non-LTE and/or 3D effects may affect the determination from the CH absorption features. From Bonifacio et al. (2009), a star with similar parameters as G64−12 and G64−37 would have its carbon abundance decreased by $\sim$ 0.6 dex if 3D effects were taken into account. However, given that the Fe abundance is also decreased by $\sim$ 0.3 dex, the net effect on [C/Fe] would be −0.30, and both G64−12 and G64−37 would still meet the [C/Fe]$\geq$ +0.7 CEMP criterion of Aoki et al. (2007).

3. IMPLICATIONS ON FIRST-STAR NUCLEOSYNTHESIS

The chemical-abundance pattern of CEMP-no Group-II stars with [Fe/H] $<$ −3.0 is likely to be the result of one, or at most a few, supernova explosions that occured in the early Universe (Ito et al. 2013; Placco et al. 2014b, 2015), polluting the ISM of the natal clouds from which second-generation stars formed. To quantify how the previously under-estimated carbon abundances affect the inferred progenitor masses of G64−12 and G64−37, we employed the `starfit`[7] online routine, in order to compare the observed elemental abundances with an extensive grid of non-rotating massive-star models of primordial composition from Heger & Woosley (2010).

For the measured abundances in G64−12, the best model-fit is a progenitor with 10.9 $M_\odot$, explosion energy of 0.6 $\times$ 10^{51} erg, and a remnant mass of 1.5 $M_\odot$.

[7] http://starfit.org

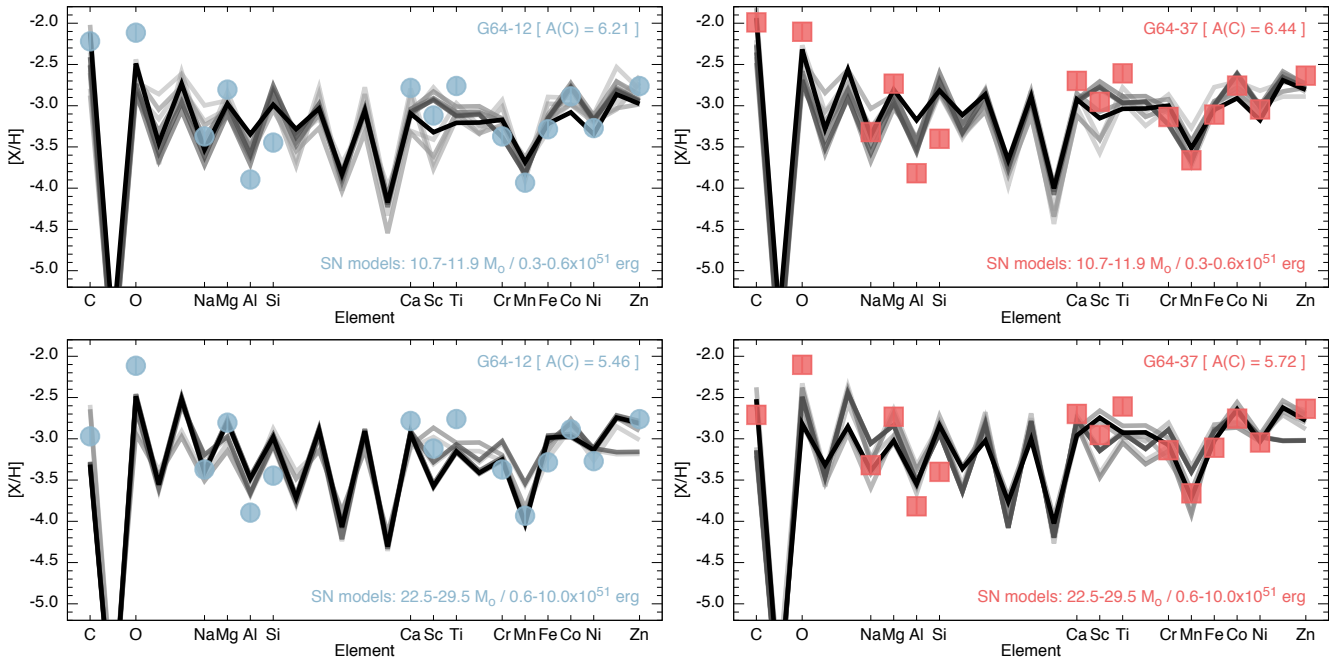
G64-12 [A(C) = 6.21]
SN models: 10.7-11.9 M$_o$ / 0.3-0.6x10^{51} erg
G64-37 [A(C) = 6.44]
SN models: 10.7-11.9 M$_o$ / 0.3-0.6x10^{51} erg
G64-12 [A(C) = 5.46]
SN models: 22.5-29.5 M$_o$ / 0.6-10.0x10^{51} erg
G64-37 [A(C) = 5.72]
SN models: 22.5-29.5 M$_o$ / 0.6-10.0x10^{51} erg
[X/H]
-2.0
-2.5
-3.0
-3.5
-4.0
-4.5
-5.0
C O NaMg Al Si Ca Sc Ti Cr Mn Fe Co Ni Zn
Element

Figure 3. Best model fits for G64−12 (left panels) and G64−37 (right panels), using the carbon abundances measured by Reggiani et al. (2016) (top panels) and the ones from the literature (lower panels). The filled symbols represent the observed abundances in Table 1, and the solid lines show the yields for the 10 best models fits in each case, with the mass and explosion energy ranges listed in the lower right part of each panel.

If the lowest previous carbon-abundance measurement for G64−12 is used as an input (A(C) = 5.46[8] ; Barklem et al. 2005), the best model-fit would be a progenitor with 29.5 $M_\odot$, explosion energy of 10×10^{51} erg, and a remnant mass of 1.7 $M_\odot$. For G64−37, the best model-fits for the measured abundances is a progenitor with 10.9 $M_\odot$, explosion energy of 0.6×10^{51} erg, and a remnant mass of 1.4 $M_\odot$. Using the carbon abundance measured by Akerman et al. (2004, A(C) = 5.72, and roughly the same $T_{\rm eff}$), the progenitor is best described by the model with 22.5 $M_\odot$, explosion energy of 10×10^{51} erg, and a remnant mass of 1.6 $M_\odot$.

Figure 3 shows the result of the model-fitting exercise, following the abundance sampling procedure described in Roederer et al. (2016) and Placco et al. (2016). The left panels show the results for G64−12, and the right panels for G64−37. The upper and lower panels show the fits for the different carbon abundances listed above. The measured abundances are represented by the filled symbols, and the solid lines represent the yields for the 10 best model-fits (i.e., lowest residuals between model and observations), with the mass and explosion energy ranges listed in the lower right part of each panel.

From Figure 3, it can be seen that the overall agreement is similar for the different carbon abundances, with the exception of Al and Si, which are over-produced by the models in the case of higher carbon abundances. Thus, the carbon-abundance measurements for both of these stars impacts estimates of their progenitor masses, by factors of $\sim 2-3$ (lower for lower A(C)). The effect on the predicted explosion energies is greater still, on the order of $\sim 10-15$ (higher for lower A(C)), sufficient to affect interpretation of the nature of the progenitors. Our new estimates are consistent with "faint" mixing-and-fallback supernovae (e.g.; Heger & Woosley 2010; Nomoto et al. 2013, and references therein).

There are also implications for derivation of the frequency of CEMP-no stars as a function of metallicity, which provides an important constraint for Galactic chemical evolution models (Lee et al. 2013; Placco et al. 2014a). Stars with effective temperatures near the main-sequence turnoff, such as G64−12 and G64−37, which are numerous in extant large samples of CEMP stars such as those from the Sloan Digital Sky Survey (York et al. 2000), could easily be mis-classified as carbon-normal stars, resulting in a spurious reduction in their derived frequencies. This is particularly the case for frequencies based on low- to medium-resolution spectroscopy of limited S/N ratios. Lee et al. (2013) quantified this effect, and found that for stars with [Fe/H]< -2.5, the fraction of CEMP stars was 32% for their giant sample, 10% for turnoff stars, and 15% for main-sequence stars. This effect is attributed to difficulties in measuring carbon abundances at high temperatures, since the average carbon abundance for a given population of stars should not depend on their evolutionary status, once proper corrections are taken into account (see Placco et al. 2014a, for further details).

For samples with carbon abundances measured in high-resolution, there is an opposite trend. From the SAGA Database (Suda et al. 2008), using stars with [Fe/H]< -3.0 and carbon measurements (excluding upper limits), there are 202 stars with $T_{\rm eff}< 5750$ K and 58 stars with $T_{\rm eff}\geq 5750$ K. For the latter $T_{\rm eff}$ range, 52% of the stars are CEMP, in contrast with the overall fraction

[8] The quoted value in Barklem et al. (2005) is A(C) = 5.66, with a measured temperature of $T_{\rm eff}$= 6141 K. To roughly account for the $\sim$ 400 K difference in temperature with respect to the present work, we re-derived the carbon abundance using a model atmosphere with the stellar parameters from Barklem et al., and the measured value decreased by 0.2 dex. We then applied this offset to the quoted value, yielding A(C)=5.46.

of 43% given by Placco et al. (2014a). This is yet another consequence of the difficulty of measuring carbon at high temperatures, which in this case introduces a bias towards higher values, which can still be measured at lower S/N ratios. In addition, the percentage of reported upper limits in carbon abundances increases from 5% for stars with [Fe/H] < -3.0 and $T_{\rm eff} < 5750$ K, to 34% for stars with $T_{\rm eff} \geq 5750$ K (most with upper limits [C/Fe] $> +1.0$). Higher S/N data for such stars is clearly desirable, and will change the CEMP frequencies currently reported. We note, in passing, that the star SDSS J102915+172927 ([Fe/H] ~ -5.0; Caffau et al. 2011), an ultra metal-poor star with $T_{\rm eff} \sim 5800$ K and only an upper limit on its carbon abundance, may fall into this category. If a carbon enhancement is confirmed for this star, it would increase the CEMP fractions from 80% to 100% for [Fe/H]≤ -5.0.

4. CONCLUSIONS

In this letter we have provided conclusive evidence that the well-known and extensively studied EMP subdwarfs G64−12 and G64−37 are in fact CEMP-no Group-II stars, based on high-resolution, extremely high signal-to-noise data from KECK/HIRES. Both are members of the outer-halo population and are single stars, properties that have been demonstrated to be associated with CEMP-no stars (Carollo et al. 2014; Hansen et al. 2016). Many more examples of warm CEMP-no stars near the halo main-sequence turnoff that have been previously claimed as carbon-normal stars are likely to be found in future investigations. We have also shown that underestimates of the carbon abundances for such stars can have large affects on the inferred progenitor masses and explosion energies of CEMP-no stars. Future studies of the frequencies of CEMP-no stars as a function of metallicity will need to consider this result as well; existing frequency estimates based on samples including stars with effective temperatures $\gtrsim$ 5750 K likely under-estimate the true fractions of CEMP-no stars.

We thank Johannes Andersen, Tadafumi Matsuno, and the anonymous referee, for providing insightful comments on the manuscript. V.M.P. and T.C.B. acknowledge partial support for this work from the National Science Foundation under Grant No. PHY-1430152 (JINA Center for the Evolution of the Elements). H.R. acknowledges support from the CAPES fellowship program. J.M. acknowledges support from FAPESP (2012/24392-2) and CNPq (Bolsa de Produtividade). This research has made use of NASA's Astrophysics Data System Bibliographic Services; the `arXiv` pre-print server operated by Cornell University (http://arxiv.org/); the SIMBAD database hosted by the Strasbourg Astronomical Data Center; the IRAF software packages distributed by the National Optical Astronomy Observatories, which are operated by AURA, under cooperative agreement with the NSF (http://iraf.noao.edu/); the SAGA Database (Stellar Abundances for Galactic Archeology; Suda et al. 2008); the `R-project` software package (https://www.r-project.org/); the `gnuplot` command-line plotting program; and the `stackoverflow` online Q&A platform (http://stackoverflow.com/).

REFERENCES

Akerman, C. J., Carigi, L., Nissen, P. E., Pettini, M., & Asplund, M. 2004, A&A, 414, 931
Allen, C., Poveda, A., & Schuster, W. J. 1991, A&A, 244, 280
Aoki, W., Beers, T. C., Christlieb, N., et al. 2007, ApJ, 655, 492
Aoki, W., Frebel, A., Christlieb, N., et al. 2006, ApJ, 639, 897
Asplund, M., Grevesse, N., Sauval, A. J., & Scott, P. 2009, ARA&A, 47, 481
Barklem, P. S., Christlieb, N., Beers, T. C., et al. 2005, A&A, 439, 129
Beers, T. C., & Christlieb, N. 2005, ARA&A, 43, 531
Beers, T. C., Preston, G. W., & Shectman, S. A. 1992, AJ, 103, 1987
Beers, T. C., Carollo, D., Ivezić, Ž., et al. 2012, ApJ, 746, 34
Bidelman, W. P. 1956, Vistas in Astronomy, 2, 1428
Bonifacio, P., Spite, M., Cayrel, R., et al. 2009, A&A, 501, 519
Bonifacio, P., Caffau, E., Spite, M., et al. 2015, A&A, 579, A28
Caffau, E., Bonifacio, P., François, P., et al. 2011, Nature, 477, 67
Carney, B. W., Laird, J. B., & Latham, D. W. 1988, AJ, 96, 560
Carollo, D., Freeman, K., Beers, T. C., et al. 2014, ApJ, 788, 180
Carollo, D., Beers, T. C., Lee, Y. S., et al. 2007, Nature, 450, 1020
Fabbian, D., Nissen, P. E., Asplund, M., Pettini, M., & Akerman, C. 2009, A&A, 500, 1143
Frebel, A., Johnson, J. L., & Bromm, V. 2007, MNRAS, 380, L40
Frebel, A., & Norris, J. E. 2015, ARA&A, 53, 631
Hansen, T. T., Andersen, J., Nordström, B., et al. 2016, A&A, 586, A160
Heger, A., & Woosley, S. E. 2010, ApJ, 724, 341
Hoyle, F. 1954, ApJS, 1, 121
Ito, H., Aoki, W., Beers, T. C., et al. 2013, ApJ, 773, 33
Kamijo, F. 1959, PASJ, 11, 257
Keenan, P. C. 1942, ApJ, 96, 101
Latham, D. W., Stefanik, R. P., Torres, G., et al. 2002, AJ, 124, 1144
Lee, Y. S., Beers, T. C., Masseron, T., et al. 2013, AJ, 146, 132
Masseron, T., Plez, B., Van Eck, S., et al. 2014, A&A, 571, A47
Meléndez, J., Schuster, W. J., Silva, J. S., et al. 2010, A&A, 522, A98
Nissen, P. E., Akerman, C., Asplund, M., et al. 2007, A&A, 469, 319
Nomoto, K., Kobayashi, C., & Tominaga, N. 2013, ARA&A, 51, 457
Nomoto, K., Nakamura, T., & Kobayashi, C. 1999, Ap&SS, 265, 37
Peterson, R. C., & Sneden, C. 1978, ApJ, 225, 913
Placco, V. M., Frebel, A., Beers, T. C., Chan, C., & Heger, A. 2016, ApJ, 999
Placco, V. M., Frebel, A., Beers, T. C., & Stancliffe, R. J. 2014a, ApJ, 797, 21
Placco, V. M., Frebel, A., Lee, Y. S., et al. 2015, ApJ, 809, 136
Placco, V. M., Kennedy, C. R., Beers, T. C., et al. 2011, AJ, 142, 188
Placco, V. M., Beers, T. C., Roederer, I. U., et al. 2014b, ApJ, 790, 34
Puget, J. L., & Heyvaerts, J. 1980, A&A, 83, L10
Ramírez, I., Meléndez, J., Bean, J., et al. 2014, A&A, 572, A48
Reggiani, H., Meléndez, J., Yong, D., Ramírez, I., & Asplund, M. 2016, A&A, 586, A67
Roederer, I. U., Placco, V. M., & Beers, T. C. 2016, ApJ, 824, L19
Ross, F. E. 1930, AJ, 40, 38
Sandage, A. 1969, ApJ, 158, 1115
Sneden, C. A. 1973, PhD thesis, The University of Texas at Austin.
Spite, M., Caffau, E., Bonifacio, P., et al. 2013, A&A, 552, A107
Suda, T., Katsuta, Y., Yamada, S., et al. 2008, PASJ, 60, 1159
Yoon, J., Beers, T. C., Placco, V. M., et al. 2016, ArXiv e-prints, arXiv:1607.06336
York, D. G., Adelman, J., Anderson, Jr., J. E., et al. 2000, AJ, 120, 1579
Zhang, L., Karlsson, T., Christlieb, N., et al. 2011, A&A, 528, A92